ECOLOGY

Self-organized mud cracking amplifies the resilience of an iconic "Red Beach" salt marsh

Kang Zhang[1,2]†, Jiaguo Yan[2,3,4,5]†, Qiang He[6], Chi Xu[7,8]*, Johan van de Koppel[2,9], Bo Wang[7], Baoshan Cui[3]*, Quan-Xing Liu[1,10]

Self-organized patterning, resulting from the interplay of biological and physical processes, is widespread in nature. Studies have suggested that biologically triggered self-organization can amplify ecosystem resilience. However, if purely physical forms of self-organization play a similar role remains unknown. Desiccation soil cracking is a typical physical form of self-organization in coastal salt marshes and other ecosystems. Here, we show that physically self-organized mud cracking was an important facilitating process for the establishment of seepweeds in a "Red Beach" salt marsh in China. Transient mud cracks can promote plant survivorship by trapping seeds, and enhance germination and growth by increasing water infiltration in the soil, thus facilitating the formation of a persistent salt marsh landscape. Cracks can help the salt marsh withstand more intense droughts, leading to postponed collapse and faster recovery. These are indications of enhanced resilience. Our work highlights that self-organized landscapes sculpted by physical agents can play a critical role in ecosystem dynamics and resilience to climate change.

INTRODUCTION

A wide variety of ecosystems form spatially regular patterns, as has been observed in the past decades in arid vegetation (*1*–*4*), peatlands (*5*, *6*), mussel beds (*7*–*9*), and salt marsh ecosystems (*10*–*12*). The patterns are explained by a self-organization process, where patterns develop through the interactions between organisms and their environments, e.g., salt marsh vegetation locally influencing hydrodynamic forces and sedimentation, leading to the formation of clustered patterning of vegetation with power-law–like patch-size distributions (*10*). Mathematical models highlight the importance of self-organized spatial patterns and other forms of spatial complexity in determining the resilience of these ecosystems to climate change, maintaining ecosystem integrity, and allowing gradual, reversible transitions in ecosystems that would face harsh tipping behavior if not for adaptive capacity emerging from the self-organization processes (*10*, *13*–*15*).

Many ecosystems show ordered spatial structures that cannot be explained solely by biologically triggered self-organization (see Table 1 for a summary). In addition, physical systems, without partial biological mediation, can form ordered spatial patterns (*16*–*21*). Well-known examples include dune systems in deserts (*22*) and rock patterns in arctic environments (*16*). Specifically, physical spatial patterns (see Fig. 1 for examples) increase the complexity of ecosystems by strengthening the spatial redistribution of water and soil resources at microhabitat scales and decreasing (or increasing) hydrological connectivity between ecosystems (*4*, *20*, *23*). However, the importance of physical patterns of self-organization for maintaining the integrity of the world's ecosystems facing climate change is for the most an unstudied topic.

Here, we focus on coastal salt marshes, where biologically triggered self-organization in various forms has been extensively studied. We report a physical self-organization in the form of drought-mediating crack formation on tidal mudflats, facilitating ecosystem resilience to droughts. Desiccation cracks emerging in the surficial sediment layer are a widespread phenomenon in coastal salt marshes and other wetland ecosystems (Figs. 1 and 2). Induced by drying, the continuous surface of sediments will split to form cracks that extend downward into the sublayers, exhibiting polygons with relatively regular sizes on the surface (Fig. 2A). The physical processes of crack formation have been studied using laboratory experiments and finite element analytical models (*24*–*29*). In real-world ecosystems, once the cracks are formed, plants are often observed to colonize within the cracks (Figs. 1 and 2). This process plausibly invokes interactions between seed germination (and/or plant growth) and this special geomorphological feature. So far, such plant-crack interactions have not been considered in existing crack modeling framework (*27*), and we know very little if and how geometric configuration of crack patterns is related with the interplay of biotic and abiotic interactions therein.

In this study, we used high-resolution drone photos in combination with detailed in situ manipulative experiments to study the underlying mechanism of crack formation and how it influences plant establishment and growth in a salt marsh ecosystem in the Yellow River Delta, northern China (see Methods and fig. S1 for details). The seepweed *Suaeda salsa* (*Suaeda* hereafter) is an euhalophyte

[1]Center for Global Change and Complex Ecosystems, School of Ecological and Environmental Sciences, East China Normal University, Shanghai 200241, China. [2]Department of Estuarine and Delta Systems, Royal Netherlands Institute of Sea Research, Yerseke 4401 NT, The Netherlands. [3]State Key Joint Laboratory of Environmental Simulation and Pollution Control, School of Environment, Beijing Normal University, Beijing 100875, China. [4]Wuxi Research Institute of Applied Technologies, Tsinghua University, Wuxi 214072, China. [5]Division of Oilfield Chemicals, China Oilfield Services Limited (COSL), Beijing, China. [6]Coastal Ecology Lab, National Observation and Research Station for Shanghai Yangtze Estuarine Wetland Ecosystems, School of Life Sciences, Fudan University, 2005 Songhu Road, Shanghai 200438, China. [7]School of Life Sciences, Nanjing University, Nanjing 210023, China. [8]Breeding Base for State Key Laboratory of Land Degradation and Ecological Restoration in northwestern China; Key Laboratory of Restoration and Reconstruction of Degraded Ecosystems in northwestern China of Ministry of Education, Ningxia University, Yinchuan 750021, China. [9]Groningen Institute for Evolutionary Life Sciences, Conservation Ecology Group, University of Groningen, Groningen 9700 CC, The Netherlands. [10]School of Mathematical Sciences, Shanghai Jiao Tong University, Shanghai 200240, China.
†These authors contributed equally to this work.
*Corresponding author. Email: xuchi@nju.edu.cn (C.X.); cuibs@bnu.edu.cn (B.C.)

Table 1. Physical patterns observed in diverse ecosystems. These examples include patterns originated from purely physical processes and geomorphic physical patterns created by animals.

Ecosystem	Patterning mechanism	Ecological functions	Reference/ location
Salt marsh	Desiccation cracks induced by drying	Seed trapping, water entrapment, and enhanced plant performance	Fig. 2; the present study
Lake	Salt ridges driven by evaporation	Breeding habitats for flamingos	Fig. 1A
Floodplain wetland	Movements of megafauna species	Drainage channel and nutrition transport	(*79*)
Grassland	Livestock trampling	Water redistribution on slopes	(*23*)
Dryland	Desiccation cracks induced by drying	Facilitating plant survival in winters and springs; plant feedbacks to soils.	Fig. 1, B and C; Hanksville, UT; Atacama Desert, Chile

species with high salt tolerance, which grows on intertidal and supratidal (hyper-)saline soils (*30*). Its seeds are dispersed (or passively entrained) by water flow and then germinate in favorable environmental conditions. Massive salt marshes dominated by *Suaeda* form iconic "Red Beach" landscapes that often invoke awe and attract tourists. They are also rich in ecological functions (*31*), providing critical habitats for many migratory birds and important ecosystem services to humans (*32*, *33*). Large-scale degradation of *Suaeda* salt marshes induced by droughts and reclamation has been observed in many critical coastal ecosystems (*33*–*35*). Restoring these valuable degraded ecosystems has been identified as a priority of coastal restoration.

We proposed a mathematical model to understand how drought-induced physical self-organization generates mud cracks facilitating and interacting with the crack-living species *Suaeda*, triggering the emergence of a transient ecosystem state that ultimately leads to the recovery of the highly valued Red Beach salt marshes in northern China (*33*). We further show how this self-organized system responds to environmental stress such as drought events and maintains productivity at the landscape scale. Our results suggest that crack patterns resulting from sediment contraction can trigger a physical self-organization process, enhance the resilience of coastal ecosystems to droughts, and maintain the ecosystem service of salt marshes in terms of coast protection. In a general sense, our work highlights the importance of physical self-organization in supporting ecosystem structure, functioning, and resilience.

RESULTS

Field observations and experiments

In coastal salt marshes, it is common to find spatial patterns characterized by network-like mud cracks interleaved with polygons (typical size of ca. 0.85 m^2 in our study site; Fig. 2, B to D). Mud cracks are especially abundant after drought events. We first conducted detailed field survey to examine if and how the *Suaeda* plants and the crack patterns are correlated. Our field observation showed that the *Suaeda* plants were predominantly present within the cracks (Fig. 2). Moreover, once plant clusters were formed, they can alter local hydrodynamic forces to amplify sediment erosion in the places where the plants grow, in turn facilitating the persistence of the cracks (Fig. 2, B and D). This observed positive plant-crack association may be seen as a sign of ecosystem engineering (*27*, *36*), leading us to propose a working hypothesis that a positive plant-crack feedback underlies the system.

We conducted four in situ experiments to test this hypothesis (see Methods and Table 2 for details). Our result from experiment 1 (see Table 2) based on a factorial design in terms of presence/absence of cracks showed that the soils were softer within cracks than inside polygonal patches without cracks ($F_{3,44}$ = 215.4, P < 0.001; Fig. 3A), and plant growth can further soften the soils (Tukey post hoc test, P < 0.001, n = 12; Fig. 3A). The presence of cracks and plants can decrease soil hardness by ca. 20 and 30%, respectively (Fig. 3A). Soil salinity and dryness (inverse of soil water content) showed similar responses with soil hardness to the presence of cracks and plants (for salinity, $F_{3,44}$ = 28.6, P < 0.001; Fig. 3B; for soil water, $F_{3,44}$ = 23.6, P < 0.001; Fig. 3C). These results indicate that both cracks and plants can improve soil conditions by decreasing soil hardness and salinity and enhancing soil water

Table 2. Field experiments testing the feedback mechanism between mud cracks and *Suaeda* plants.

Experiment	Treatment	Description
Experiment 1: Effects of plant and cracks on soil conditions	Crack (+), Plant (+)	Both the cracks and plants were present.
	Crack (–), Plant (+)	The cracks were compacted, but the plants were retained.
	Crack (+), Plant (–)	The cracks were retained, but the plants were removed.
	Crack (–), Plant (–)	The cracks were compacted, and the plants were removed.
Experiment 2: Effect of plants on crack persistence	High plant density	Ten seedling individuals were transplanted.
	Medium plant density	Five seedling individuals were transplanted.
	Plant removal	Existing plants were removed.
Experiment 3: Effect of cracks on seed entrapment	–	Number of germinated seedlings in relation to crack width.
Experiment 4: Effects of cracks on plant survivorship	With crack	Seedlings were transplanted into cracks.
	Crack compacted	Seedlings were transplanted into cracks, and then cracks were compacted.
	Patch center	Seedlings were transplanted at crack-formed patch centers.
	Intermediate location	Seedlings were transplanted into locations between cracks and patch centers.
	Control	Seedlings in the pretransplantation area.

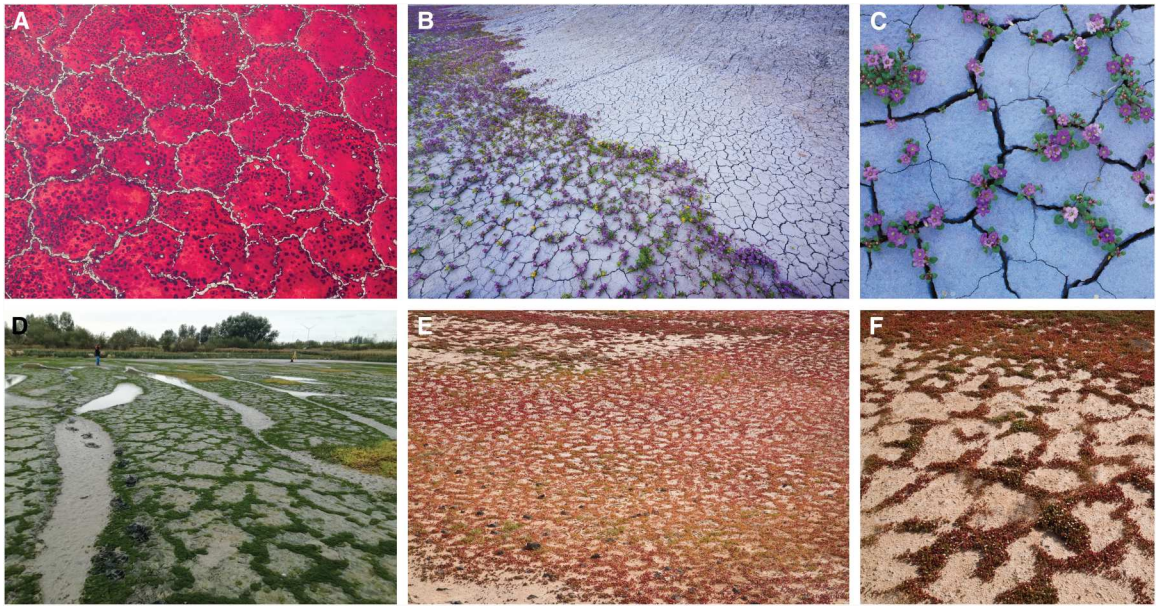

Fig. 1. Examples of cracking patterns in different ecosystems. (**A**) Cracking pattern with red algae and salt formations in shallow salt waters of Lake Natron, Tanzania, Africa. Photo credit: Danita Delimont/Alamy Stock Photo. (**B**) Flowering Phacelia (*Phacelia sabulonum*) and beeplants (*Cleome lutea*) growing out of soil cracks after a shower (Factory Bench, Fremont, UT, USA). (**C**) Zoom in of (B). Photo credit for (B) and (C): Guy Tal. (**D**) Spatial pattern of mud cracks and Vaucheria (fibrous green benthic algae) growing in the cracks in the coastal ecosystem in Ketenisse, Schelde Estuary, Belgium. Photo credit: Greg Fivash. (**E**) Slenderleaf iceplant (*Mesembryanthemum nodiflorum*) growing in the mud cracks in saltpan, Salinas de Janubio, Lanzarote, Spain. (**F**) Zoom in of (E). Photo credit: Bob Gibbons/Alamy Stock Photo.

availability. Facilitated by the presence of cracks, the plants showed higher total biomass ($P < 0.05$) and allocated less below-ground biomass ($P < 0.01$) (Fig. 3F).

We also examined the effect of crack width on seed entrapment (measured by the number of germinated seedlings) and seedling survivorship (experiments 3 and 4; Table 2 and fig. S4). Our results showed that the number of germinated seedlings had a positive linear relationship with crack width ($R^2 = 0.83$, $P < 0.001$; Fig. 3D and table S1) and that the survival of transplanted plants within cracks declined more slowly over time than in the no-crack treatments (Fig. 3E). Notably, plant individuals transplanted into the bare patch centers (without crack formation) presented the lowest survival compared with other treatments (Fig. 3E). These experimental results suggest that cracks can effectively alleviate the unfavorable soil conditions for plant establishment, facilitating plant survival and growth.

Our experiments (experiments 1 and 2; Table 2) also indicate a positive effect of plants on cracks. The presence of plants was associated with crack widths about twofold higher than the no-plant treatments (experiment 1; fig. S5A). The existence of transplanted plants can effectively maintain the persistence of the cracks and enlarge the cracks over the entire growing season, whereas the removal of plants resulted in quick disappearance of cracks (experiment 2; fig. S5B).

Together, our results from the field experiments converge to support the hypothesis that a positive feedback exists between plants and mud cracks, plausibly leading to a spontaneous (re)colonization and self-maintenance process of salt marsh vegetation. Framed in a general sense, it creates a self-organization process on (either primary or secondary) bare mudflats: The hypersaline and arid soil conditions plausibly preclude the colonization of other plant species that are not as tolerant as *Suaeda*, and the high soil hardness also largely precludes the establishment of *Suaeda* in bare patches when cracks are absent. Under these conditions representing a critical bottleneck for plants, mud cracks can arise as induced by droughts. This is followed by *Suaeda* germinating, surviving, and growing out of the cracks under suitable conditions; once established, *Suaeda* vegetation can sustain itself through the aforementioned crack-plant interactions that help alleviate the environmental stress. In our study site, we did not observe apparent vegetative expansion of *Suaeda* into bare patches without the presence of cracks, probably because of the absence of lateral expansion ability of *Suaeda* (although our short-term observations cannot completely exclude this possibility).

The theoretical model and crack network formation

To further test whether this self-organization underlies the observed landscape pattern and system dynamics, we built a spatially continuous mean-field model (see Methods for details) incorporating the aforementioned key processes (Fig. 4, A and B). Specifically, the mathematical model is grounded on the experimental evidence that plant growth depends on soil water content and soil hardness represented by local tensile stress of soil surface (variable S). In the model, water content in the soil sublayer (variable W) is consumed by plants (variable P) and is dependent on humidity of the soil surface layer (variable E) and evaporation. We use a bilinear function to describe local soil surface layer humidity in relation to sublayer soil water content and air saturated humidity (Eq. 1c). For local tensile stress, a bistable states function with a critical tensile stress (S_{cri}) is typically taken (Eq. 1a) to describe the process that a crack forms when tensile stress goes beyond the critical value and shifts to an alternative state (*37*, *38*).

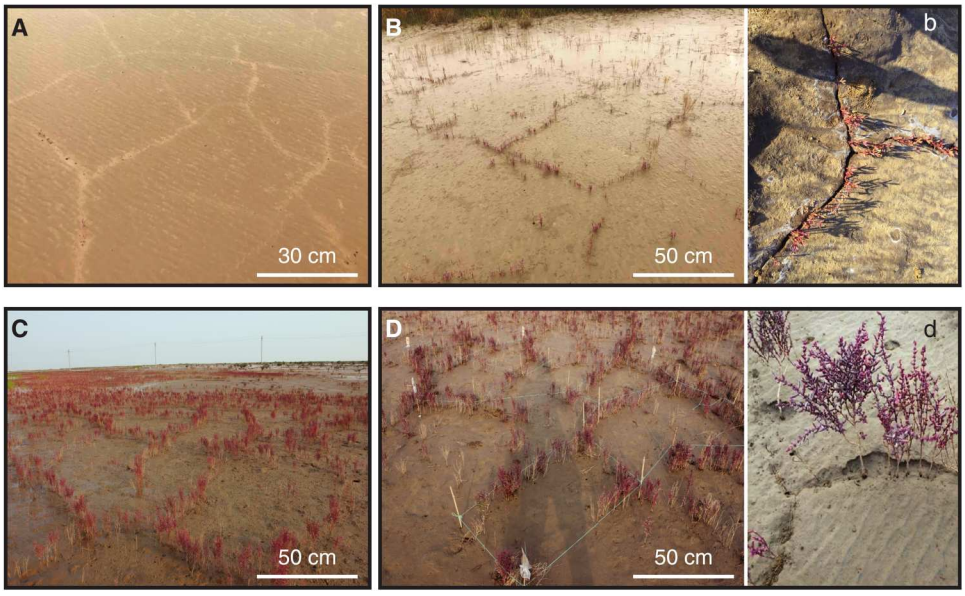

Fig. 2. Network-like mud cracking patterns and distribution of annual plant *Suaeda salsa* in the study site. (**A**) Cracks formed before *Suaeda* establishment. (**B**) *Suaeda* seedling growing out of the cracks at start of growing season (**b** as a zoom-in panel). (**C**) *Suaeda* vegetation pattern in the peak season. (**D**) Field measurement of crack pattern characteristics (**d** as a zoom-in panel showing clustered plants associated with an enlarged crack). Photo credit: Jiaguo Yan.

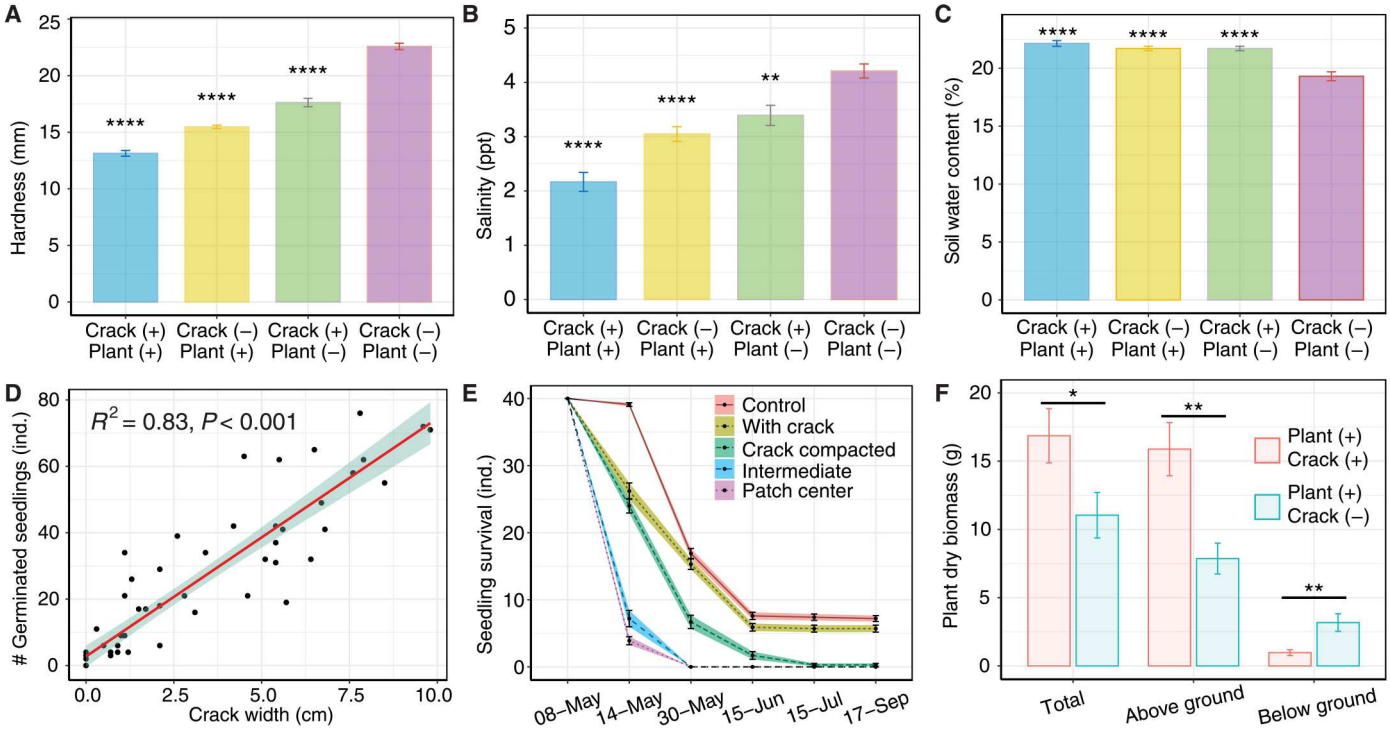

Fig. 3. In situ experiments examining plant-crack interactions. Soil hardness (**A**), salinity (**B**), and water content (**C**) for the four treatments with respect to the presence/absence of cracks and *Suaeda* plants in experiment 1 (mean ± SE, $n = 12$). (**D**) Positive relationship between crack width and number of germinated *Suaeda* seedlings revealed by experiment 2 (regression line and 95% confidence interval are shown). (**E**) Seedlings survivorship over time for the five treatments in experiment 4. (**F**) Plant biomass in the treatment with versus without cracks in experiment 1. See Methods, figs. S4 and S5, Table 2, and table S1 for more details. ***$P < 0.001$, **$P < 0.01$, and *$P < 0.05$ [compared with Crack (–), Plant (–) in (A) to (C)].

We modeled the spatial variation of the focal variables in a two-dimensional space (Fig. 4, C to F). Our model well captures the anti-phase behavior between local tensile stress and plant biomass (Fig. 4C), in line with the positive response of mud cracks to plant growth and seed germination. As expected, plant biomass displays a spatial synchronous distribution associated with sublayer soil water content. Similarly, in Fig. 4 (D to F), we describe the development of the two-dimensional patterns of tensile stress, water content, and plants starting from a random initial condition. In addition, our model also captures "dangled" and "isolated" cracks (i.e., single cracks that are partially or not connected with the crack network). These types of cracks can be commonly observed in coastal salt marshes and many other ecosystems (see Table 1) but have not been well reflected in typical finite element models.

Modeled versus observed landscape patterns

We used drone photos at 3.5 cm spatial resolution to quantify the geometric properties of the crack networks and associated patches at the landscape scale and compared the drone-derived empirical properties with the model-derived counterparts (Fig. 5, A and B). In particular, we looked at five geometrical parameters, i.e., angle, average patch length, perimeter, area, and circularity (defined as the ratio of a patch's area to the area of a circle whose perimeter is equal to that of the patch; see Methods), which have been commonly used in previous studies (*37*, *38*).

Our comparison demonstrates that the observed landscape cracking pattern is highly consistent with the modeled pattern, in terms of the distributions of these five geometrical parameters. First, the observed and modeled patterns have highly consistent joint distributions of crack angle and length, with 90° angle as the dominant mode (Fig. 5, C and F). Second, the patch perimeter–area relationship scales consistently across the landscape in a way independent of the scale of analysis (Fig. 5, D and G, and tables S2 and S3). This scale-free relation is seen as a spatial self-similarity property (*18*). The revealed scaling law (with an exponent of ca. 0.53) thus highlights the emergent self-affine property resulting from the spatial self-organization process. Third, the joint distribution of patch circularity and area is also consistent between the observed and modeled patterns, with an area mode around 0.85 m^2 and circularity mode around 0.77 (Fig. 5, E and H).

We also assessed the model performance at a larger scale, with a clear spatial gradient of soil water content. In the study area, soil water content substantially declines with increasing distance from the creeks (fig. S7). This gradient can be well reflected in our model as well (Fig. 6, A and B, and fig. S8).

Ecosystem resilience enhanced by self-organized cracking

Both our field experiments and modeling results indicate that the physically self-organized mud cracks can provide a critical shelter for *Suaeda* with improved soil conditions, creating or amplifying the window of opportunity for *Suaeda* vegetation. An intuitive corollary from these results is that self-organized cracking can enhance ecosystem resilience. We then tested this idea by examining the modeled system behavior in terms of ecological and engineering resilience to droughts (*39*). Our model analysis suggests that in the absence of self-organized cracks, ecosystem tipping points would occur with abrupt vegetation collapse (Fig. 6C). However, self-organized cracking can result in a wider bistable range, indicating a "postponed" tipping point at the system-wide scale (thus representing higher ecological resilience), as compared with the system absent of self-organized cracking (see the difference between the bifurcation point positions on the black curves in Fig. 6C versus Fig. 6D). When the self-organization is present, some local areas may follow a different trajectory characterized by slower (nonabrupt)

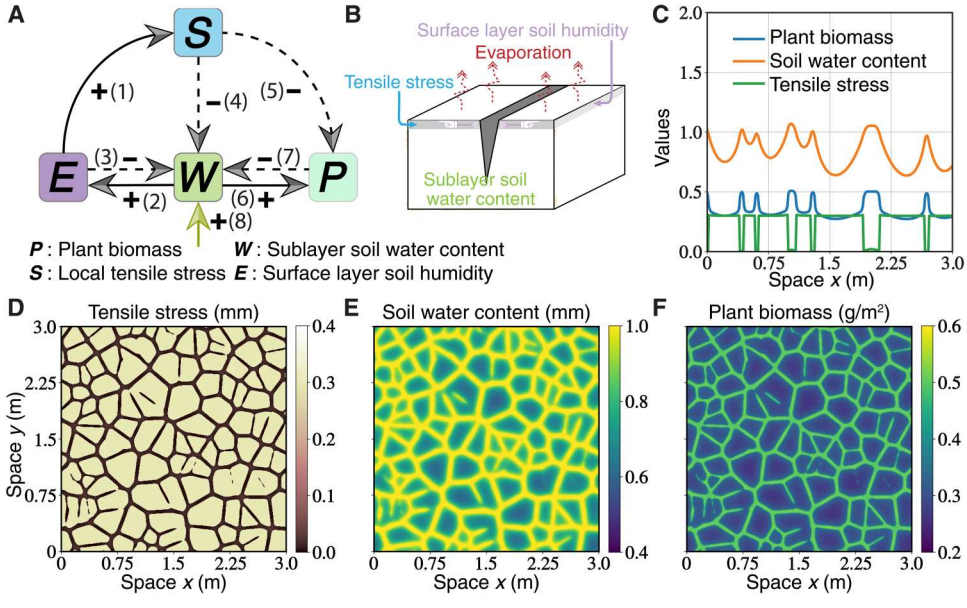

Fig. 4. Theoretical model for self-organized crack patterns. (**A**) Illustration of the positive (solid arrows with "+") and negative (dashed arrows with "–") interactions among the four key variables considered in the model. The numbers within brackets indicate the essential processes denoted in Eq. 1 in Methods. (**B**) Illustration of crack formation induced by tensile stress change depending on soil water and evaporation (red arrows). (**C**) One-dimensional and (**D** to **F**) two-dimensional patterns derived from the model. The one-dimensional curves in (C) were plotted by taking a random horizontal line from (D) to (F). Note that lowest tensile stress describes a fracture state here (0 PMa). See table S4 for model parameters. See movies S1 and S2 for numerical simulations of system dynamics.

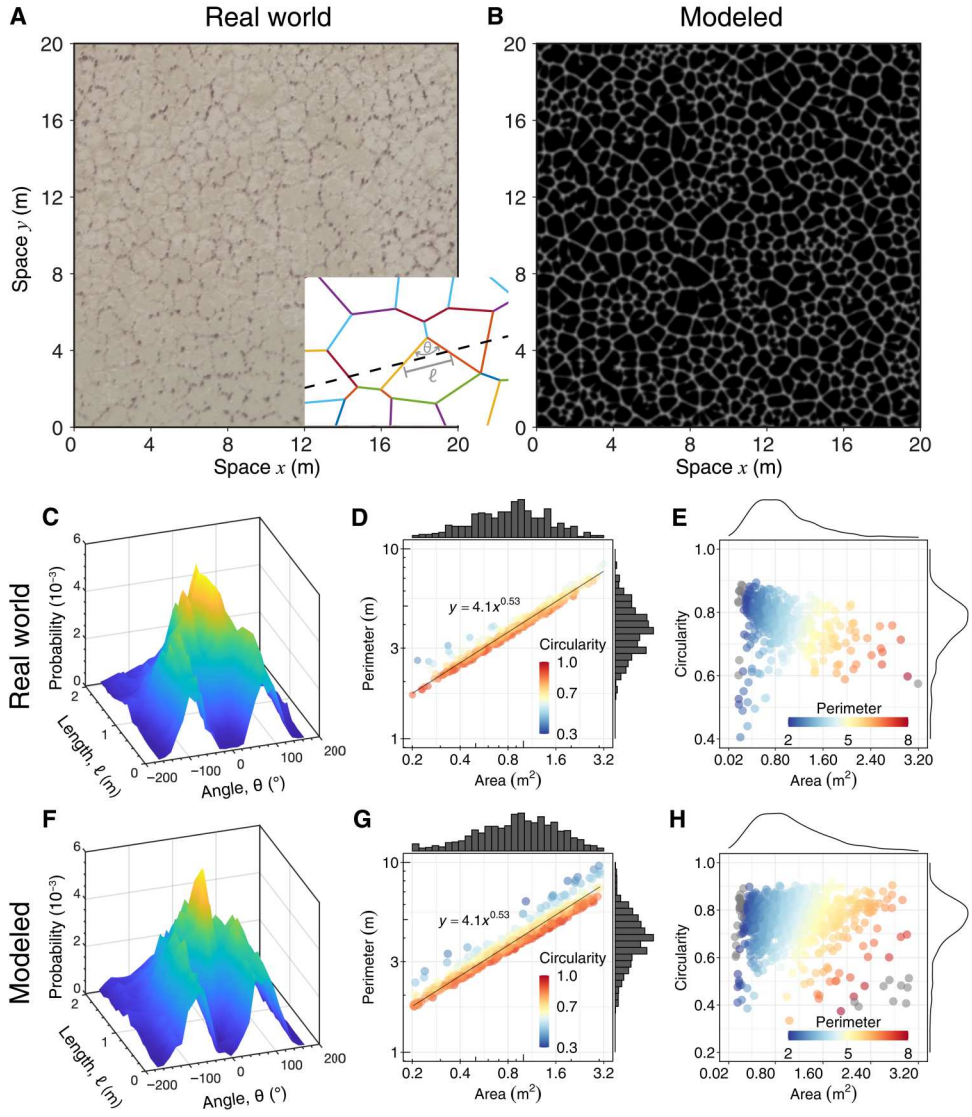

Fig. 5. Characteristics of the real-world versus modeled crack patterns. (**A**) Drone snapshot of the study site showing the crack patterns. (**B**) Crack pattern produced by the theoretical model. Probability distributions of crack spacing length ℓ and angle θ for the (**C**) real-world and (**F**) modeled crack patterns. ℓ and θ are measured on the basis of 1000 random sampling lines as illustrated in the inset of (A). Distributions and relationships between patch area and perimeter of crack-formed polygons for the (**D**) real-world and (**G**) modeled patterns. Distributions of patch area and circularity of crack-formed polygons for the (**E**) real-world and (**H**) modeled patterns. See Methods and tables S2 and S3 for details.

decline of vegetation biomass (see the blue curves in Fig. 6D for maximum local vegetation biomass), suggesting that these local subsystems may "evade" the tipping point at the system-wide level (*13*).

We also conducted a perturbation experiment in the model to assess how physically self-organized mud cracks could affect vegetation recovery rate upon perturbations as a straightforward indicator of engineering resilience. To this end, we constructed a spatially homogeneous (nonpatterned, without self-organized cracking) landscape that have the same model parameters as the patterned system (with self-organized cracking). We removed 60% of vegetation biomass from the nonpatterned and patterned systems and then calculated the time that the systems require to return to equilibria. Our result showed that the patterned system with self-organized cracking presented about twofold faster recovery to equilibrium than the spatially homogeneous system without self-organized cracking (Fig. 6, E and F). In addition, the vegetation biomass of the system without self-organized cracking declines to an equilibrium that is ca. 25% lower than that with self-organized cracking after the same perturbations (Fig. 6, E and F).

Overall, our model predicts that the physically self-organized cracking can amplify the resilience of the salt marsh to droughts. This amplifies the theoretical prediction that self-organization in general can enhance the resilience of many different types of ecosystems (*7*, *10*, *13*, *40*).

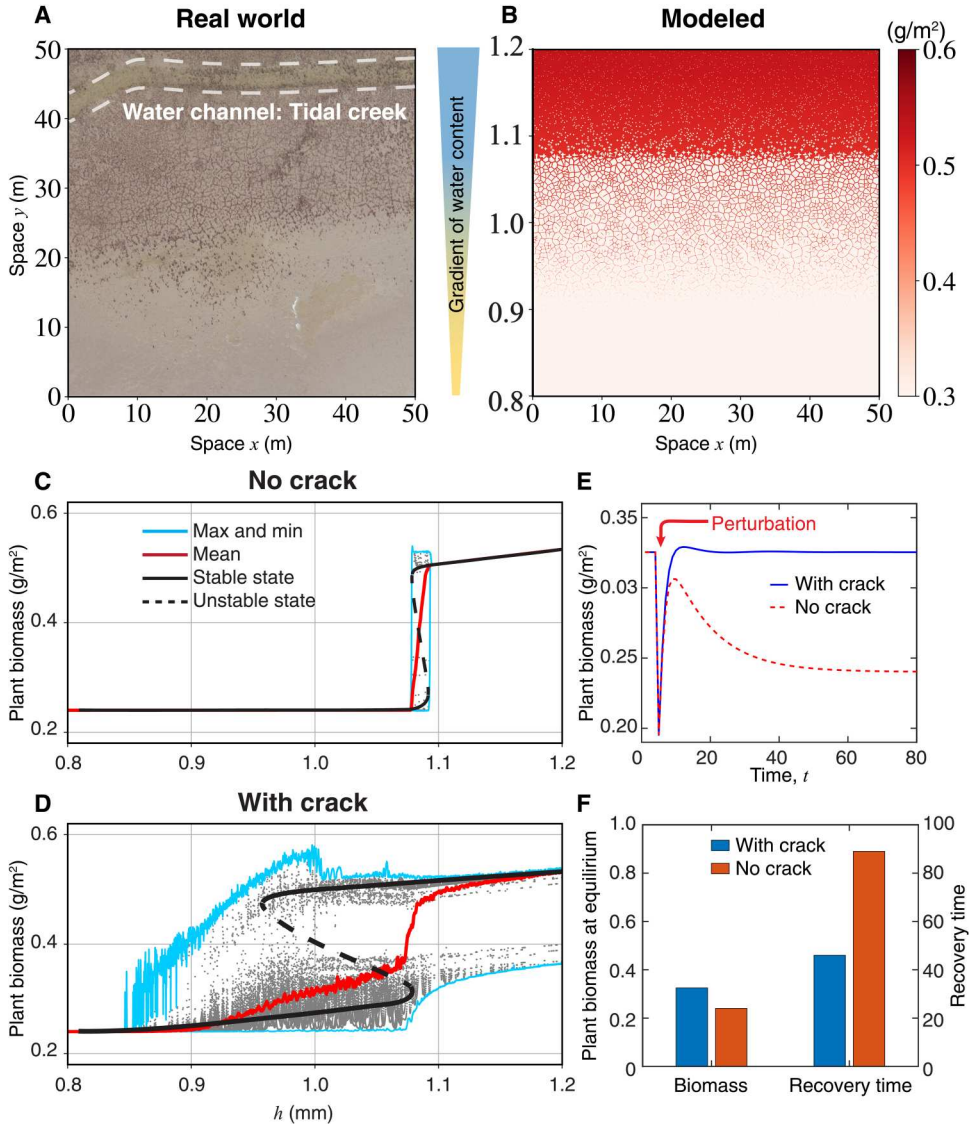

Fig. 6. Effect of self-organized mud cracks on ecosystem resilience. (**A**) A drone image shows vegetation patterns associated with mud cracks along the spatial gradient of soil water content. The upper dashed lines mark a tidal creek. A gradient of decreasing soil water content is present with increasing distance to the tidal creek (see fig. S7). (**B**) Modeled vegetation and crack patterns along a spatial gradient of soil water content (see movies S3). (**C**) In the absence of self-organized cracks, the modeled ecosystem displays tipping points with a narrow hysteresis range with changing environmental stress in terms of parameter *h* (see Eq. 1c and table S4). (**D**) Compared with the no-crack system in (C), self-organized cracking results in a postponed tipping point of ecosystem collapse at a lower threshold of environmental stress and a wider hysteresis range. The solid and dashed black lines approximately represent the locations of stable and unstable states, respectively. Some local subsystem [gray dots correspond to grid cells in (B), with blue curves showing the max/min values at a given *h*] may evade the tipping point. (**E**) Recovery trajectories of systems with versus without self-organized crack patterns following removal of 60% biomass. (**F**) Recovery time and biomass at equilibrium ($\mathscr{P}_e$) of two modeled systems in (E). See figs. S9 and S10 for supplementary results.

DISCUSSION

In this article, we explored the physically self-organized mud cracking patterns and their interactions with the *Suaeda* plants in the coastal salt marsh. Our study demonstrates that physical self-organization of mud cracks can promote the seed bank, enhance the survivorship, and facilitate the growth of the plants. These effects are attributed to redistributions of surface and soil water and ameliorated soil conditions at the microhabitat scale. The transient cracking patterns are normally activated by drought events that could induce massive vegetation die-off. However, once activated, these cracking patterns can facilitate plant (re-)establishment across the landscape, creating important positive feedbacks that eventually improve the ecosystem functioning of the salt marsh and increase its resilience to droughts. In addition, in spatially heterogeneous landscapes (*41*, *42*), this mechanism may help a fraction of local areas evade drought-induced tipping points (*13*).

Spatially self-organized patterns are ubiquitous in nature, resulting from diverse mechanisms involving environmental factors (*41*, *42*), functional morphology (*43*), developmental constraints, and optimal delivery (*18*). Most existing studies have focused on the

role of biologically triggered self-organization processes, suggesting that these processes can act as a precursor for ecosystem establishment, for instance, in water-limited (*3*, *41*, *42*) or disturbance-dominated ecosystems (*44*–*48*). While biological and physical processes are often entangled with each other in the establishment and development of self-organized ecosystems, in some particular cases, they are clearly separated—purely physical processes can first create patterns and other forms of heterogeneity as "physical templates" for ecosystems [for instance, stone aggregation on the ground as driven by frost upheaval and ice needles in arctic ecosystems (*16*, *49*)], followed by biological processes (such as plant establishment) operating upon such templates. While mechanisms underlying purely physical self-organizations have attracted much interest (*11*, *50*–*52*), their connections to ecosystem functioning and resilience have been mostly understudied. Here, we show that salt marsh mud cracking as a purely physical form of self-organization can create or expand the window of opportunity for vegetation establishment and increase ecosystem resilience to droughts (Fig. 6, C and D). Our work thus highlights that in contrast to the well-studied biologically triggered self-organization, purely physical self-organization processes in themselves can act as a precursor for ecosystem establishment.

Coastal salt marshes are shaped by complex biotic and abiotic processes involving, for instance, dispersal, environmental heterogeneity, vegetation zonation, and interspecific interactions (*53*–*55*). Clearly, we need to embed physical self-organization (of mud cracking) in the context of these fundamental ecological processes for a complete understanding of coastal ecosystem dynamics. It seems unlikely that mud cracking plays a universally predominant role across a wide range of ecosystem types and spatial scales, as its occurrence and strength is likely context-dependent. First, it is likely dependent on environmental context. We found that the facilitative effect of mud cracks by ameliorating soil water conditions is critical in high marshes subject to drying. This effect may be weak or entirely absent in other intertidal settings. For instance, mud cracks may not form or (if formed) have only minor influences on plants in low marshes, where more frequent inundations (less drying) are present and intensive wave impacts often act as the limiting factor for plant establishment and growth (*53*). Second, the occurrence and effect of mud cracks are dependent on biotic context such as species life history traits and species associations. Mud cracks appear important to the annual species *Suaeda* with a relatively low colonization ability (due to shallow and sparse roots) but maybe less so to other marsh halophyte species with higher colonization abilities. For instance, in some cases, bare mudflats without cracks can be colonized by cordgrasses and reeds through vegetative expansion (*56*). For these species, vegetation patterns may be weakly or not associated with mud cracks even if they were present. In addition, many salt marsh plants have relatively low seed dispersal abilities (*57*). They may not be dependent on cracks, but rather on the occurrence of maternal plants, dispersing vegetatively. Our study site is dominated by a single plant species, *Suaeda*, but for systems with two or more coexisting foundation species, it is not impossible that interspecific interactions outweigh the effect of mud cracks. Third, the facilitative effect of mud cracks was observed on the short term. It may, however, become irrelevant over longer time periods. For instance, Wang *et al.* (*58*) showed that cordgrass invasion can result in soil desalination across a large part of tidal flats, leading to the *Suaeda* vegetation being encroached and eventually replaced by high-elevation reeds. In this case, the long-term fate of *Suaeda* Red Beach is not determined by mud cracking.

Together, our findings may be largely restricted to the condition that mud cracks can alleviate water limitation (or other stress) as a bottleneck of vegetation establishment. Nonetheless, understanding physically self-organized mud cracking has important realistic implications for the conservation of *Suaeda* Red Beach ecosystems that are prevalent along the Chinese coast and many other similar ecosystems, especially in the face of accelerating climate change. While the physical self-organization of mud cracking studied here cannot be straightforwardly generalized to other systems and to larger scales, our work paves the way for unraveling more complex ecological processes in heterogeneous systems using thoughtful experiments and well-designed models.

In addition, our theoretical model sheds insight into the formation of many other interesting crack patterns (*26*, *29*, *59*). So far, most (if not all) existing models of cracking patterns are either numerical fracture models coupling transient heat and mass transfer [for instance, the Walder and Hallet model (*59*) describing cracks in frozen soils and rocks] or continuum phase-field models describing brittle fractures based on the traditional equations of linear elasticity (*60*–*63*). However, theoretical models integrating physical self-organizing ecological processes remain scarce, despite that a number of experimental studies have highlighted the significance of these entangled processes (*25*, *26*, *64*–*67*). Our theoretical model allows tailoring an integrated framework coupling physical patterns and biological processes for answering a range of relevant questions toward understanding complex ecosystems. Going beyond salt marsh ecosystems, our modeling framework helps to unravel other biological morphogenesis and system behaviors with biophysical self-organization patterning (as exemplified in Table 1 and Fig. 1).

In summary, our paper adds to a growing body of studies that highlight the importance of spatial self-organization in countering or preventing tipping behavior in ecosystems facing climate change (*13*–*16*, *68*). We reveal that purely physical forms of self-organization can play an equally important role as biologically triggered self-organization in shaping ecosystem resilience, especially when climate-induced stress has all but removed the organisms defining the pristine state. Hence, physical self-organization will play a crucial role in ecosystem recovery, preventing irreversibility (Fig. 6), and reducing the long-term impact of climate-induced ecosystem collapse. Our study thereby calls for more detailed investigations of physical forms of self-organization in natural systems and its importance for the biota and for ecosystem resilience.

METHODS

Study site

Our study site represents a high marsh ecosystem in the Yellow River Delta, northern China (37°49′23″N, 119°4′36″E; fig. S1). The temperate monsoon climate conditions are characterized by dry autumns, winters and springs, and rainy summers. The mean annual temperature is 14.0°C and the mean annual precipitation is 576.1 mm during 1982–2019 (fig. S3). Irregular semidiurnal microtides with a mean tidal amplitude of 1.1 to 1.5 m are present in this coastal region (*35*). Our study site is located within the core zone of the Yellow River Delta National Nature Reserve, which accommodates one of the largest native salt marshes in northern

China. Human activities are strictly forbidden in the reserve. The high marsh has a low tidal flood frequency of 1 to 15% in terms of number of days per year (*69*). The soils are characterized by a hypersaline condition with salinity of up to 25 parts per thousand and present accumulated salts on the surfaces regularly (*69*, *70*). The salt marshes are primarily dominated by the annual succulent plant species *Suaeda*. *Salicornia europaea*, *Phragmites australis*, *Tamarix chinensis*, and the invasive cordgrass *Spartina alterniflora* are also found in the Yellow River Delta (*71*). The vegetation in our study site is monospecific (*Suaeda*), presenting a sparse vegetation cover around 5% (*70*). Regular spatial patterning of *Suaeda* vegetation following self-organized mud cracking is clearly observed in the field (Fig. 2).

The Yellow River Delta was affected by recurrent droughts over the recent decades. For example, the drought event between November 2010 and February 2011 was particularly severe. A total precipitation of 27.3 mm occurred between March and May 2011 during the period of *Suaeda* seedling establishment, which was only 27% of the long-term average (*34*). It has been documented that droughts can have a strong impact on the *Suaeda* marshes, reducing vegetation cover by ca. 50% (*33*).

In situ experiments on soil conditions

To test our hypothesis that a positive feedback occurs between *Suaeda* plants and mud cracks, we conducted in situ experiments in a 150× 50 m^2 plot with relatively homogeneous biotic and abiotic conditions. The first one is a full factorial experiment investigating the effects of cracks and plants on soil conditions (see experiment 1 in Table 2 and fig. S4). For the treatments with respect to cracks, we randomly selected naturally generated cracks in the field and then randomly picked up half of these cracks to artificially compact them. These compacted cracks thus represented the "Crack (−)" treatments, and the rest untouched ones represented the "Crack (+)" treatments (Fig. 3, A to C). For the treatments with respect to plants, we removed the existing plants (both aboveground and belowground parts) to represent the "Plant (−)" treatments. We set up 12 replicates for each of the four treatments (summarized in Table 2). The experiment was conducted between 7 July and 21 December 2015. At the end of the experiment, for each replicate, we collected the aboveground and belowground biomass of all plants and then weighed their dry biomass in the laboratory (Fig. 3F). We also measured soil hardness (using the soil hardness meter SHM-22, Japan), soil salinity, and soil water content (Fig. 3, B and C), as well as crack width (fig. S5A).

In situ experiment on crack persistence

We conducted the second field experiment to test whether plant growth could affect crack persistence (see experiment 2 in Table 2). To this end, we transplanted 10 and 5 *Suaeda* seedlings, respectively, into soil cracks with a uniform length of 10 cm at the start of the growing season (May 2015), representing the high and medium seedling densities observed in the field. We also removed the existing plants within the soil cracks as a control treatment. Therefore, we have three treatments (i.e., high density, medium density, and control), each of which has 10 replicates. We monitored the crack widths monthly from June 2015 to January 2016, a whole experiment time period of 30 weeks (fig. S5B).

Seed germination experiment

We conducted a seed germination experiment to test whether mud cracks can trap plant seeds, thereby facilitating seedling establishment (see experiment 3 in Table 2). To this end, we collected the soil samples (10 cm length and 15 cm depth) within the cracks in the field in May 2015. We then took the soil samples back to greenhouse and placed them in pots. After 4 weeks, we counted the number of germinated seedlings to produce seedlings. We collected 41 samples within cracks and 20 samples outside cracks. We measured the crack width for each soil sample and examined the correlation between number of geminated seedlings and crack width (Fig. 3D; crack width was set to 0 for samples outside cracks).

In situ experiment on seedling survivorship

We conducted a transplanting experiment to test the effect of cracks on seedling survivorship (see experiment 4 in Table 2). To this end, we transplanted 40 plant seedlings together with the soil blocks that the seedlings grew on (each 10 cm in length). Our experimental treatments were set with respect to crack conditions: (i) "with crack": the transplantation was conducted with the cracks unchanged; (ii) "crack compacted": the cracks were compacted immediately after the transplantation; (iii) "patch center": the transplantation was conducted at the center of the crack-formed patch, where a bare state without existing plants was present; (iv) "intermediate location": the transplantation was conducted at the location between patch center and cracks; and (v) "control": existing plants growing within cracks. See fig. S4 for an illustration of the treatments. We used 10 replicates for each treatment. We monitored the seedling survival from 8 May to 17 September 2015, a whole experiment time period of 4 months (Fig. 3E).

Image processing and characterizations of crack patterns

We obtained aerial images in the experiment area in October 2018. The high-resolution images (ca. 3.5 cm) were taken with a DJI Phantom 4 Pro drone. The raw images were geometrically corrected and then converted to a binary raster format for the subsequent extraction of mud cracks using the image processing method by Liu *et al.* (*72*, *73*) (fig. S6). The extracted cracks were converted to the polyline format. We quantified crack spacing length (ℓ) and angle (θ) following Plug and Werner (*37*) (Fig. 5, A, C, and F). To this end, we randomly laid out 1000 sampling lines onto the extracted crack network graph. We then calculated every ℓ and θ associated with the intersecting sampling lines and cracks (see Fig. 5A, note that the isolated cracks were discarded in this calculation) to plot the joint probability distribution (Fig. 5C). Moreover, we calculated the perimeter (P_i) and area (A_i) and, on this basis, calculated circularity of each crack-formed polygon. Circularity [$C_i = \frac{A_i}{\pi\left(\frac{P_i}{2\pi}\right)^2}$] is defined as the ratio between the true area A_i and the area of the equivalent circle for the polygon (i.e., the denominator); therefore, a circularity close to 1 represents that the polygon is close to the shape of circles. We showed the scatter plot of area (A_i) versus perimeter (P_i) (Fig. 5D) and that of area (A_i) versus circularity (C_i) (Fig. 5E) for the observed crack pattern. Using the same methods, we generated these plots for the model-derived crack patterns correspondingly (Fig. 5, F to H).

Statistical analysis

We used one-way analysis of variance (ANOVA) with Tukey post hoc multiple comparisons to compare the experimental treatments. The statistical analyses were carried out using the R studio software (*74*). Between-treatment differences are labeled as $^{***}P < 0.001$, $^{**}P < 0.01$, $^{*}P < 0.05$, and "NS" for $P > 0.05$. Pearson's correlation test was used to examine the correlation between crack width and seedling number.

Mathematical model

We propose a mathematical model to provide a mechanistic understanding of spatial patterning of mud cracks and vegetation observed in the field (Fig. 2). We aim at building a simple model to reflect the underlying mechanism in a most transparent way. Regarding that our focus is spatial self-organization, our simple model is meant to reflect the fundamental processes of drying-induced crack formation and its interaction with plant establishment, which are particularly relevant for the physical self-organization of cracking patterns. We expect to use this simple model to analyze system properties such as resilience in a straightforward way. We also expect that the simple modeling framework can be adapted to study other similar systems (such as those in Fig. 1).

Our model is grounded on our field observations and experimental results that provide critical empirical bases for considering crack-plant interactions. It is built upon existing soil cracking models. However, unlike the classic finite element cracking models based on the Griffith criteria of fracture (*25*, *75*, *76*), our model is based on partial differential equations describing tensile stress with an alternative stable state driven by interstitial humidity of soil surfaces. When a crack opens, it releases stored strain energy to the environment (so that the tensile stress becomes zero). We consider a two-layer framework for modeling soil conditions, i.e., a thin surface layer where increasing tensile stress to a certain threshold can give rise to cracks, and a sublayer where the soil water is consumed by plants roots. $S(\boldsymbol{r}, t)$, $E(\boldsymbol{r}, t)$, $W(\boldsymbol{r}, t)$, and $P(\boldsymbol{r}, t)$ denote the tensile stress of soil surface layer, humidity of soil surface layer, sublayer soil water content, and plant biomass at position $\boldsymbol{r} = (x, y)$ and time t, respectively. We consider the nonlinear dynamics of tensile stress (crack states) across the fractured soil surface layer (Fig. 4, A and B) as

$$\frac{\partial S(\boldsymbol{r},t)}{\partial t} = \underbrace{r_s(S-S_{\min})(S_{\mathrm{cri}}-S)(S-S_{\max})}_{\text{Bistable states of tensile stress}} + \underbrace{c_s(E-e)}_{\text{(1) Humidity effect on tensile stress}} \tag{1a}$$

The first term describes the bistable states of tensile stress (unit of megapascal) with critical instable state of S_{cri}, where the tensile stress increases with rate r_s through connected neighbors; $S_{\min}$ and $S_{\max}$ represent the fracture and nonfracture states, respectively. The second term accounts for the positive effect on tensile stress due to evaporation. Parameter e describes the saturation value of air humidity above the soil surfaces. The positive effect on tensile stress is proportional to the net difference between soil surface layer humidity and saturated air humidity with the coefficient c_s. Note that here the interaction between soil surface layer humidity and tensile stress is spatially homogeneous.

Water content of soil sublayer is determined by the balance between water influx, water loss due to evaporation, and water depletion by plants at a given location, described as

$$\frac{\partial W(\boldsymbol{r},t)}{\partial t} = \underbrace{\frac{c_w}{k_w+S}}_{\text{(4) Water storage in cracks}} - \underbrace{d_E(E-e)W}_{\text{(3) Loss due to evaporation}} - \underbrace{l_pP\frac{W}{k_p+W}}_{\text{(7) Depletion by plants}} + \underbrace{D_w\nabla^2 W}_{\text{Diffusion}} \tag{1b}$$

where $W(\boldsymbol{r}, t)$ denotes sublayer soil water content (unit of grams per square centimeter). Note that tensile stress has an inverse relationship with sublayer soil water content. Parameter c_w denotes the water permeability coefficient for bare soil without crack formation, and k_w represents the crack effect of promoting water entrapment. Water loss due to evaporation is the product of sublayer soil water content (W) and the net difference between humidity of soil surface layer and saturated air humidity, with a coefficient of drainage rate d_E. In addition, sublayer soil water depleted by plant uptake is described as a product of plant biomass (P) and soil water content (W). Here, l_p is the maximum water uptake by plants and k_p is the half-saturation constant of water in promoting plant growth rate. The last term represents horizontal soil water diffusion, where D_w is the diffusion coefficient (the Laplace operator, second spatial derivative, $\nabla^2 = \frac{\partial^2}{\partial x^2} + \frac{\partial^2}{\partial y^2}$).

$E(\boldsymbol{r}, t)$ represents the humidity of soil surface layer, determined by sublayer soil water content and evaporation-induced water loss (as a function of the net difference between soil surface layer humidity and saturated air humidity)

$$\frac{\partial E(\boldsymbol{r},t)}{\partial t} = \underbrace{r_E(W-h)(E-e)}_{\text{(2) Evaporation process}} + \underbrace{D_E\nabla^2 E}_{\text{Diffusion}} \tag{1c}$$

where r_E is the coefficient for humidity gain from soil sublayer and h is the threshold of sublayer soil water content at which the evaporation process stops. Similar to water diffusion in the soil sublayer, we also assume water diffusion in the soil surface sublayer, with a diffusion coefficient D_E (*77*).

Last, plant biomass $P(\boldsymbol{r}, t)$ can be described by the balance between plant growth as a function of sublayer soil water content, morality induced by intraspecific competition, and diffusion

$$\frac{\partial P(r,t)}{\partial t} = \underbrace{r_pP\frac{W(1-S)}{k_p+W}}_{\text{(5,6) Facilitation by water and crack}} - \underbrace{d_pP^2}_{\text{Intraspecific competition}} + \underbrace{D_p\nabla^2 P}_{\text{Seed dispersal}} \tag{1d}$$

The first term represents growth dynamics of plants, where r_p is the maximum growth under sufficient soil water. Cracks can facilitate plant biomass by entrapment of seeds and propagules and water. Note that the tensile stress variable S lies within the range from 0 to 1.0 ($S \in (0\ 1]$); therefore, this positive feedback is integrated into the growth dynamics in an inversed way here. The second term represents biomass loss due to intraspecific competition (for water), with a coefficient d_p. The third term represents plant biomass diffusion (species dispersal). See Fig. 4A for the specific interactions corresponding to the numbers with brackets in Eq. 1 (a to d). The definitions and units of the variables and parameters are summarized in table S4.

Note that our simple model is designed for studying monospecific systems (Fig. 5) or relatively homogeneous landscape systems (Fig. 6, A and B). Thus, the model does not take into account ecological processes such as vegetation zonation and interspecific interactions, which often play important roles in shaping tidal salt marshes at larger spatial scales or in heterogeneous landscapes. The model does not account for tidal flooding as the study site is located in high marshes with occasional flood inundation. In addition, the model does not account for sea-level rise that is critical to long-term dynamics of coastal salt marshes (*78*), because we focus on ecosystem behavior in a relatively short term. The simple model may serve as a component of a more comprehensive framework for the purpose of modeling more complex ecosystem structures and dynamics.

Model analyses

We modeled the salt marsh ecosystem with mud crack patterning by solving Eq. 1 (a to d) using in-house–developed software based on the pyOpencl Python module, implemented on the AMD Radeon Pro Vega 64X platform. First, we modeled the system dynamics in a two-dimensional space consisting of 512×512 grid cells representing 3×3 m^2 with 4 million time steps (Fig. 4). Periodic boundary condition was implemented in the model to account for the edge effect. Second, we modeled the systems in a 20×20 m^2 space, allowing for detailed characterizations of the crack patterns (Fig. 5). Third, we modeled a larger-scale system (50×50 m^2) representing a spatial gradient of sublayer soil water content, where we imposed Neumann boundary condition (Fig. 6B). Our model can give rise to alternative stable states separated by tipping points. Such system behavior hinges on positive feedbacks in general, and specifically in this case the positive feedback between plants and cracks. For modeling the system without mud cracks (Fig. 6C), we reduced the diffusion coefficient of subsurface soil water content (D_w) to prevent crack pattern formation. In this way, the stable solutions of the systems do not change (*14*), allowing us to investigate the effect of cracks. We then performed a perturbation experiment by removing 60% vegetation biomass for calculating the post-perturbation recovery time to equilibria.

Supplementary Materials

This PDF file includes:
Figs. S1 to S10
Tables S1 to S4
Legends for movies S1 to S3
Legend for data S1

Other Supplementary Material for this manuscript includes the following:
Movies S1 to S3
Data S1

REFERENCES AND NOTES

1. M. Rietkerk, S. C. Dekker, P. C. de Ruiter, J. van de Koppel, Self-organized patchiness and catastrophic shifts in ecosystems. *Science* **305**, 1926–1929 (2004).
2. M. Rietkerk, J. Van de Koppel, Regular pattern formation in real ecosystems. *Trends Ecol. Evol.* **23**, 169–175 (2008).
3. C. A. Klausmeier, Regular and irregular patterns in semiarid vegetation. *Science* **284**, 1826–1828 (1999).
4. J. A. Castillo Vardaro, J. A. Bonachela, C. C. M. Baker, M. L. Pinsky, D. F. Doak, R. M. Pringle, C. E. Tarnita, Resource availability and heterogeneity shape the self-organisation of regular spatial patterning. *Ecol. Lett.* **24**, 1880–1891 (2021).
5. D. R. Foster, G. A. King, P. H. Glaser, H. E. Wright Jr., Origin of string patterns in boreal peatlands. *Nature* **306**, 256–258 (1983).
6. M. B. Eppinga, P. C. de Ruiter, M. J. Wassen, M. Rietkerk, Nutrients and hydrology indicate the driving mechanisms of peatland surface patterning. *Am. Nat.* **173**, 803–818 (2009).
7. J. van de Koppel, J. C. Gascoigne, G. Theraulaz, M. Rietkerk, W. M. Mooij, P. M. J. Herman, Experimental evidence for spatial self-organization and its emergent effects in mussel bed ecosystems. *Science* **322**, 739–742 (2008).
8. Q.-X. Liu, A. Doelman, V. Rottschäfer, M. de Jager, P. M. J. Herman, M. Rietkerk, J. van de Koppel, Phase separation explains a new class of self-organized spatial patterns in ecological systems. *Proc. Natl. Acad. Sci. U.S.A.* **110**, 11905–11910 (2013).
9. J. van de Koppel, M. Rietkerk, N. Dankers, P. M. J. Herman, Scale-dependent feedback and regular spatial patterns in young mussel beds. *Am. Nat.* **165**, E66–E77 (2005).
10. L.-X. Zhao, K. Zhang, K. Siteur, X.-Z. Li, Q.-X. Liu, J. van de Koppel, Fairy circles reveal the resilience of self-organized salt marshes. *Sci. Adv.* **7**, eabe1100 (2021).
11. E. J. Weerman, J. van de Koppel, M. B. Eppinga, F. Montserrat, Q.-X. Liu, P. M. J. Herman, Spatial self-organization on intertidal mudflats through biophysical stress divergence. *Am. Nat.* **176**, E15–E32 (2010).
12. J. van de Koppel, D. van der Wal, J. P. Bakker, P. M. J. Herman, Self-organization and vegetation collapse in salt marsh ecosystems. *Am. Nat.* **165**, E1–E12 (2005).
13. M. Rietkerk, R. Bastiaansen, S. Banerjee, J. van de Koppel, M. Baudena, A. Doelman, Evasion of tipping in complex systems through spatial pattern formation. *Science* **374**, eabj0359 (2021).
14. Q.-X. Liu, P. M. J. Herman, W. M. Mooij, J. Huisman, M. Scheffer, H. Olff, J. van de Koppel, Pattern formation at multiple spatial scales drives the resilience of mussel bed ecosystems. *Nat. Commun.* **5**, 5234 (2014).
15. R. Bastiaansen, A. Doelman, M. B. Eppinga, M. Rietkerk, The effect of climate change on the resilience of ecosystems with adaptive spatial pattern formation. *Ecol. Lett.* **23**, 414–429 (2020).
16. A. Li, N. Matsuoka, F. Niu, J. Chen, Z. Ge, W. Hu, D. Li, B. Hallet, J. van de Koppel, N. Goldenfeld, Q.-X. Liu, Ice needles weave patterns of stones in freezing landscapes. *Proc. Natl. Acad. Sci. U.S.A.* **118**, e2110670118 (2021).
17. P. Lu, C. Narteau, Z. Dong, P. Claudin, S. Rodriguez, Z. An, L. Fernandez-Cascales, C. Gadal; Sylvain Courrech du Pont, Direct validation of dune instability theory. *Proc. Natl. Acad. Sci. U.S.A.* **118**, e2024105118 (2021).
18. I. Rodriguez-Iturbe, A. Rinaldo, *Fractal River Basins: Chance and Self-Organization* (Cambridge Univ. Press, 1997).
19. S. Fagherazzi, Self-organization of tidal deltas. *Proc. Natl. Acad. Sci. U.S.A.* **105**, 18692–18695 (2008).
20. E. Sheffer, J. von Hardenberg, H. Yizhaq, M. Shachak, E. Meron, Emerged or imposed: A theory on the role of physical templates and self-organisation for vegetation patchiness. *Ecol. Lett.* **16**, 127–139 (2013).
21. L. G. Larsen, J. W. Harvey, How vegetation and sediment transport feedbacks drive landscape change in the everglades and wetlands worldwide. *Am. Nat.* **176**, E66–E79 (2010).
22. V. C. Reijers, K. Siteur, S. Hoeks, J. van Belzen, A. C. W. Borst, J. H. T. Heusinkveld, L. L. Govers, T. J. Bouma, L. P. M. Lamers, J. van de Koppel, T. van der Heide, A Lévy expansion strategy optimizes early dune building by beach grasses. *Nat. Commun.* **10**, 2656 (2019).
23. I. Stavi, H. Yizhaq, Y. Osem, E. Argaman, Positive impacts of livestock and wild ungulate routes on functioning of dryland ecosystems. *Ecol. Evol.* **11**, 13684–13691 (2021).
24. L. Goehring, Evolving fracture patterns: Columnar joints, mud cracks and polygonal terrain. *Philos. Trans. A Math. Phys. Eng. Sci.* **371**, 20120353 (2013).
25. P. Nandakishore, L. Goehring, Crack patterns over uneven substrates. *Soft Matter* **12**, 2253–2263 (2016).
26. P. H. Morris, J. Graham, D. J. Williams, Cracking in drying soils. *Can. Geotech. J.* **29**, 263–277 (1992).
27. C.-S. Tang, C. Zhu, Q. Cheng, H. Zeng, J.-J. Xu, B.-G. Tian, B. Shi, Desiccation cracking of soils: A review of investigation approaches, underlying mechanisms, and influencing factors. *Earth Sci. Rev.* **216**, 103586 (2021).
28. S. Hirobe, K. Oguni, Modeling and numerical investigations for hierarchical pattern formation in desiccation cracking. *Physica D* **359**, 29–38 (2017).
29. A. H. Lachenbruch, Depth and spacing of tension cracks. *J. Geophys. Res.* **66**, 4273–4292 (1961).
30. Q. He, B. R. Silliman, B. S. Cui, Incorporating thresholds into understanding salinity tolerance: A study using salt-tolerant plants in salt marshes. *Ecol. Evol.* **7**, 6326–6333 (2017).
31. C. E. Studds, B. E. Kendall, N. J. Murray, H. B. Wilson, D. I. Rogers, R. S. Clemens, K. Gosbell, C. J. Hassell, R. Jessop, D. S. Melville, D. A. Milton, C. D. T. Minton, H. P. Possingham, A. C. Riegen, P. Straw, E. J. Woehler, R. A. Fuller, Rapid population decline in migratory shorebirds relying on Yellow Sea tidal mudflats as stopover sites. *Nat. Commun.* **8**, 14895 (2017).
32. F. Shi, D. Weaver, Y. Zhao, M.-F. Huang, C. Tang, Y. Liu, Toward an ecological civilization: Mass comprehensive ecotourism indications among domestic visitors to a Chinese wetland protected area. *Tour. Manag.* **70**, 59–68 (2019).

33. J. Ren, J. Chen, C. Xu, J. van de Koppel, M. S. Thomsen, S. Qiu, F. Cheng, W. Song, Q.-X. Liu, C. Xu, J. Bai, Y. Zhang, B. Cui, M. D. Bertness, B. R. Silliman, B. Li, Q. He, An invasive species erodes the performance of coastal wetland protected areas. *Sci. Adv.* **7**, eabi8943 (2021).
34. Q. He, B. R. Silliman, Z. Z. Liu, B. S. Cui, Natural enemies govern ecosystem resilience in the face of extreme droughts. *Ecol. Lett.* **20**, 194–201 (2017).
35. Q. He, A. H. Altieri, B. S. Cui, Herbivory drives zonation of stress-tolerant marsh plants. *Ecology* **96**, 1318–1328 (2015).
36. T. J. Bouma, M. B. De Vries, P. M. J. Herman, Comparing ecosystem engineering efficiency of two plant species with contrasting growth strategies. *Ecology* **91**, 2696–2704 (2010).
37. L. J. Plug, B. T. Werner, Fracture networks in frozen ground. *J. Geophys. Res. Solid Earth* **106**, 8599–8613 (2001).
38. L. J. Plug, B. T. Werner, Nonlinear dynamics of ice-wedge networks and resulting sensitivity to severe cooling events. *Nature* **417**, 929–933 (2002).
39. V. Dakos, S. Kéfi, Ecological resilience: What to measure and how. *Environ. Res. Lett.* **17**, 043003 (2022).
40. E. N. Mueller, *Patterns of Land Degradation in Drylands Understanding Self-Organised Eco-geomorphic Systems* (Springer, 2013).
41. A. I. Borthagaray, M. A. Fuentes, P. A. Marquet, Vegetation pattern formation in a fog-dependent ecosystem. *J. Theor. Biol.* **265**, 18–26 (2010).
42. C. Latorre, C. Latorre, A. L. González, J. Quade, J. M. Fariña, R. Pinto, P. A. Marquet, Establishment and formation of fog-dependent *Tillandsia landbeckii* dunes in the Atacama Desert: Evidence from radiocarbon and stable isotopes. *J. Geophys. Res. Biogeo.* **116**, G03033 (2011).
43. E.-H. M. El-Hacen, T. J. Bouma, P. Oomen, T. Piersma, H. Olff, Large-scale ecosystem engineering by flamingos and fiddler crabs on West African intertidal flats promote joint food availability. *Oikos* **128**, 753–764 (2019).
44. T. Balke, T. J. Bouma, E. M. Horstman, E. L. Webb, P. L. A. Erftemeijer, P. M. J. Herman, Windows of opportunity: Thresholds to mangrove seedling establishment on tidal flats. *Mar. Ecol. Prog. Ser.* **440**, 1–9 (2011).
45. T. Balke, P. M. J. Herman, T. J. Bouma, Critical transitions in disturbance-driven ecosystems: Identifying windows of opportunity for recovery. *J. Ecol.* **102**, 700–708 (2014).
46. T. Balke, K. Lõhmus, H. Hillebrand, O. Zielinski, K. Haynert, D. Meier, D. Hodapp, V. Minden, M. Kleyer, Experimental salt marsh islands: A model system for novel metacommunity experiments. *Estuar. Coast. Shelf Sci.* **198**, 288–298 (2017).
47. R. M. Chambers, D. T. Osgood, D. J. Bart, F. Montalto, Phragmites australis invasion and expansion in tidal wetlands: Interactions among salinity, sulfide, and hydrology. *Estuaries* **26**, 398–406 (2003).
48. Z. Hu, J. van Belzen, D. van der Wal, T. Balke, Z. B. Wang, M. Stive, T. J. Bouma, Windows of opportunity for salt marsh vegetation establishment on bare tidal flats: The importance of temporal and spatial variability in hydrodynamic forcing. *J. Geophys. Res. Biogeo.* **120**, 1450–1469 (2015).
49. M. Kessler, B. Werner, Self-organization of sorted patterned ground. *Science* **299**, 380–383 (2003).
50. B. T. Larson, T. Ruiz-Herrero, S. Lee, S. Kumar, L. Mahadevan, N. King, Biophysical principles of choanoflagellate self-organization. *Proc. Natl. Acad. Sci. U.S.A.* **117**, 1303–1311 (2020).
51. R. C. van de Vijsel, "Biophysical self-organization of coastal wetlands: Unraveling spatial complexity on tidal flats and marshes, from the Precambrian to today," thesis, University of Groningen (2021).
52. X. Dong, A. B. Murray, J. B. Heffernan, Competition among limestone depressions lads to self-organized regular patterning on a flat landscape. *J. Geophys. Res. Earth Surf.* **126**, e2021JF006072 (2021).
53. M. D. Bertness, A. M. Ellison, Determinants of pattern in a New England salt marsh plant community. *Ecol. Monogr.* **57**, 129–147 (1987).
54. A. Finotello, A. D'Alpaos, M. Marani, E. Bertuzzo, A minimalist model of salt-marsh vegetation dynamics driven by species competition and dispersal. *Front. Mar. Sci.* **9**, 866570 (2022).
55. K. Lõhmus, T. Balke, M. Kleyer, Spatial and temporal patterns of initial plant establishment in salt marsh communities. *J. Veg. Sci.* **31**, 1122–1132 (2020).
56. M. D. Bertness, Zonation of Spartina patens and Spartina alterniflora in New England salt marsh. *Ecology* **72**, 138–148 (1991).
57. E. R. Chang, R. M. Veeneklaas, J. P. Bakker, Seed dynamics linked to variability in movement of tidal water. *J. Veg. Sci.* **18**, 253–262 (2007).
58. B. Wang, K. Zhang, Q.-X. Liu, Q. He, J. van de Koppel, S. N. Teng, X. Miao, M. Liu, M. D. Bertness, C. Xu, Long-distance facilitation of coastal ecosystem structure and resilience. *Proc. Natl. Acad. Sci. U.S.A.* **119**, e2123274119 (2022).
59. J. Walder, B. Hallet, A theoretical model of the fracture of rock during freezing. *Geol. Soc. Am. Bull.* **96**, 336–346 (1985).
60. A. Karma, A. E. Lobkovsky, Unsteady crack motion and branching in a phase-field model of brittle fracture. *Phys. Rev. Lett.* **92**, 245510 (2004).
61. V. I. Marconi, E. A. Jagla, Diffuse interface approach to brittle fracture. *Phys. Rev. E Stat. Nonlin. Soft Matter. Phys.* **71**, 036110 (2005).
62. E. A. Jagla, Maturation of crack patterns. *Phys. Rev. E Stat. Nonlin. Soft Matter. Phys.* **69**, 056212 (2004).
63. L. B. Freund, *Dynamic Fracture Mechanics. Cambridge Monographs on Mechanics and Applied Mathematics* (Cambridge Univ. Press, 2009).
64. K. Toga, B. E. Alaca, Junction formation during desiccation cracking. *Phys. Rev. E Stat. Nonlin. Soft Matter. Phys.* **74**, 021405 (2006).
65. J. B. Murton, R. Peterson, J.-C. Ozouf, Bedrock fracture by ice segregation in cold regions. *Science* **314**, 1127–1129 (2006).
66. J. B. Murton, J.-P. Coutard, J.-P. Lautridou, J.-C. Ozouf, D. A. Robinson, R. B. G. Williams, Physical modelling of bedrock brecciation by ice segregation in permafrost. *Permafr. Periglac. Process.* **12**, 255–266 (2001).
67. J. B. Murton, J.-P. Coutard, J.-P. Lautridou, J.-C. Ozouf, D. A. Robinson, R. B. G. Williams, G. Guillemet, P. Simmons, Experimental design for a pilot study on bedrock weathering near the permafrost table. *Earth Surf. Process. Landf.* **25**, 1281–1294 (2000).
68. K. Siteur, E. Siero, M. B. Eppinga, J. D. M. Rademacher, A. Doelman, M. Rietkerk, Beyond turing: The response of patterned ecosystems to environmental change. *Ecol. Complex.* **20**, 81–96 (2014).
69. T. Xie, S. Li, B. Cui, J. Bai, Q. Wang, W. Shi, Rainfall variation shifts habitat suitability for seedling establishment associated with tidal inundation in salt marshes. *Ecol. Indic.* **98**, 694–703 (2019).
70. Q. Wang, T. Xie, M. Luo, J. Bai, C. Chen, Z. Ning, B. Cui, How hydrological connectivity regulates the plant recovery process in salt marshes. *J. Appl. Ecol.* **58**, 1314–1324 (2021).
71. B.-S. Cui, Q. He, Y. An, Community structure and abiotic determinants of salt marsh plant zonation vary across topographic gradients. *Estuaries Coast.* **34**, 459–469 (2011).
72. C. Liu, C.-S. Tang, B. Shi, W.-B. Suo, Automatic quantification of crack patterns by image processing. *Comput. Geosci.* **57**, 77–80 (2013).
73. C. Liu, B. Shi, J. Zhou, C. Tang, Quantification and characterization of microporosity by image processing, geometric measurement and statistical methods: Application on SEM images of clay materials. *Appl. Clay Sci.* **54**, 97–106 (2011).
74. R Core Team, *R: A Language and Environment for Statistical Computing* (R Foundation for Statistical Computing, 2022); www.R-project.org.
75. B. R. Lawn, *Fracture of Brittle Solids. Cambridge Solid State Science Series* (Cambridge Univ. Press, 2010).
76. T. Bai, D. D. Pollard, H. Gao, Explanation for fracture spacing in layered materials. *Nature* **403**, 753–756 (2000).
77. C. K. Ballantyne, *Periglacial Geomorphology* (Wiley Blackwell, 2018).
78. A. D. Campbell, L. Fatoyinbo, L. Goldberg, D. Lagomasino, Global hotspots of salt marsh change and carbon emissions. *Nature* **612**, 701–706 (2022).
79. P. Gwin, "Why the wildebeest is the unlikely king of the Serengeti," *National Geographic*, 30 November 2021, pp. 34–45.

Acknowledgments: We thank three anonymous reviewers for their valuable comments on earlier versions of this paper. We thank J. Ren for providing the drone images and remotely sensed land cover maps. We thank G. Tal for permitting the use of the pictures in Fig. 1 (B and C). **Funding:** This work was supported by the National Key R&D Program of China (2022YFF1301000), the Key Project of National Natural Science Foundation of China (grant nos. U2243208 and U1901212), and the Science and Technology Commission of Shanghai Municipality (grant no. 18dz2271000). C.X. acknowledges the support from the National Natural Science Foundation of China (grant no. 32061143014) and the Open Fund for Key Laboratory of Land Degradation and Ecological Restoration in northwestern China of Ningxia University (grant no. LDER2023Z01). J.Y. acknowledges the support from the National Natural Science Foundation of China (grant no. 51909005). K.Z. acknowledges the support from ECNU Academic Innovation Promotion Program for Excellent Doctoral Students (grant no. YBNLTS2021-030). **Author contributions:** Q.-X.L., J.v.d.K., C.X., and B.C. designed research. K.Z. and Q.-X.L. developed the model. K.Z. performed simulation. J.Y. and J.v.d.K. designed experiments. J.Y. performed experiments. K.Z., J.Y., B.W., C.X., and Q.-X.L. performed data analyses. Q.H. carried out drone image collection. Q.-X.L., C.X., and J.v.d.K. interpreted results and wrote the manuscript with input from all coauthors. **Competing interests:** The authors declare that they have no competing interests. **Data and materials availability:** All data needed to evaluate the conclusions in the paper are present in the paper and/or the Supplementary Materials. The code used in this study is publicly available at https://doi.org/10.6084/m9.figshare.22237327.v1.

Submitted 2 April 2022
Accepted 30 March 2023
Published 3 May 2023
10.1126/sciadv.abq3520